Los Alamos NATIONAL LABORATORY EST.1943

LA-UR-18-29312 (Accepted Manuscript)

Verification and Validation of the FLAG Hydrocode for Impact Cratering Simulations

Caldwell, Wendy Kaye
Hunter, Abigail
Plesko, Catherine Suzanne
Wirkus, Stephen

Provided by the author(s) and the Los Alamos National Laboratory (2019-03-21).

To be published in: Journal of Verification, Validation and Uncertainty Quantification

DOI to publisher's version: 10.1115/1.4042516

Permalink to record: http://permalink.lanl.gov/object/view?what=info:lanl-repo/lareport/LA-UR-18-29312

Disclaimer:
Approved for public release. Los Alamos National Laboratory, an affirmative action/equal opportunity employer, is operated by the Los Alamos National Security, LLC for the National Nuclear Security Administration of the U.S. Department of Energy under contract DE-AC52-06NA25396. Los Alamos National Laboratory strongly supports academic freedom and a researcher's right to publish; as an institution, however, the Laboratory does not endorse the viewpoint of a publication or guarantee its technical correctness.

RESEARCH LIBRARY

Verification and Validation of the FLAG Hydrocode for Impact Cratering Simulations

Wendy K. Caldwell[1,2,†], Abigail Hunter[1], Catherine S. Plesko[1], Stephen Wirkus[3]

[1] X-Computational Division, Los Alamos National Laboratory, Los Alamos, NM 87545
[2] School of Mathematical and Statistical Sciences, Arizona State University, Tempe, AZ 85281
[3] School of Mathematical and Natural Sciences, Arizona State University, Glendale, AZ 85306
[†] wkcaldwell@lanl.gov

Abstract

Verification and validation (V&V) are necessary processes to ensure accuracy of the computational methods used to solve problems key to vast numbers of applications and industries. Simulations are essential for addressing impact cratering problems, because these problems often exceed experimental capabilities. Here we show that the FLAG hydrocode, developed at Los Alamos National Laboratory, can be used for impact cratering simulations by verifying FLAG against two analytical models of aluminum-on-aluminum impacts at different impact velocities and validating FLAG against a glass-into-water laboratory impact experiment. Our verification results show good agreement with the theoretical maximum pressures, with relative errors as low in magnitude as 1.00%. Our validation results demonstrate FLAG's ability to model various stages of impact cratering, with crater radius relative errors as low as 3.48% and crater depth relative errors as low as 0.79%. Our mesh resolution study shows that FLAG converges at resolutions low enough to reduce the required computation time from about 28 hours to about 25 minutes. We anticipate that FLAG can be used to model larger impact cratering problems with increased accuracy and decreased computational cost on current systems relative to other hydrocodes tested by Pierazzo et al. [30].

1 Introduction

Impacts have had a lasting impression on the solar system since its beginning. Evidence of impacts exists in the numerous craters that cover the solid bodies in the solar system [21]. Closer to home, approximately 50 meteroids with diameters greater than 10 cm enter Earth's atmosphere daily, while those with diameters greater than 2 m enter the atmosphere several times per year [8]. Most of these smaller objects disintegrate in the atmosphere [8]. Objects with diameters larger than 20 m have the potential to cause substantial damage through megaton-scale airbursts. These objects enter the atmosphere about once per century [8]. Objects with the potential to have catastrophic effects occur less frequently: every 1000 years for objects with diameters around 100 m; every 100,000 years for objects with diameters around 1 km; every 100 million years for objects with diameters around 10 km [2, 26]. Artificial impact missions such as Deep Impact and the Lunar Crater Observation Sensing Satellite (LCROSS) have provided insight into the impact cratering process, allowing observations of ejecta, impact plumes, temperature, and crater dimensions [1,19]. The forthcoming Double Asteroid Redirection Test (DART) mission will test kinetic impactor asteroid deflection by impacting Didymos-B with a 500 kg impactor at an impact velocity of about 6 km/s and measuring the resulting change in orbital period [35]. However, missions of this nature occur infrequently, and the spatial scale of these problems prohibits experimentation. As a result,

scientists must rely on numerical methods to study impact cratering.

The process of forming impact craters can be divided into three stages: contact and compression; excavation; modification. The initial stage involves the impact of the projectile with the surface, resulting in a transfer of energy and momentum. The materials in the target and projectile compress, resulting in shock waves [27]. During excavation, the shock wave expands through the target material, weakening into an elastic wave. Target material may be vaporized, creating a vapor plume affecting any surrounding atmosphere, or projected out of the crater, creating an ejecta blanket [27]. During the modification stage, debris ceases to flow up and out of the crater and instead flows downward toward the center of the crater, known as crater collapse [27]. The ability to accurately model these stages opens the door to investigate many outstanding questions about our universe such as the ages of target surfaces, erosion on target surfaces, relative ages of different geologic features, and duration of crater retention [17, 31]. However, one of the only measures of accuracy we have to compare model results is through comparison to the geometry of the craters left following impacts from solid projectiles, although mineral phases can provide insight into pressure history if samples are available. As seen from the formation process, crater size and geometry depend on many factors, among them the size, velocity, and composition of the impactor, the composition of the target, and local gravity [21]. The impact cratering process includes a strength-gravity transition. The circumstances surrounding the impact determine whether crater formation is dominated by gravity or by material strength [29]. For the latter, solid material properties are essential to understanding how impact craters form. Hence, accurate numerical simulations of impacts and the resulting craters require codes that are able to capture shock dynamics as well as model how materials react under shock conditions.

The FLAG hydrodynamics code (hydrocode) [9–11], maintained and developed at Los Alamos National Laboratory, is a multiphysics research code with access to various physics models and a diverse set of numerical methods. FLAG relies on a finite volume formulation to compute continuum mechanics solutions (namely through approximating solutions to the Euler equations) using either a staggered-grid or cell-centered hydrodynamics algorithm. FLAG utilizes a fully unstructured grid, allowing an arbitrary polyhedral mesh, that can accommodate physical processes in 1, 2, and 3 spatial dimensions [20]. Several mesh optimization methods are available such as adaptive mesh refinement (AMR), and advection through arbitrary Langrangian-Eulerian (ALE) [12]. Furthermore, FLAG is a fully parallel code, and the user can indicate the number of processors per dimension or allow FLAG to make this determination [20].

FLAG has an extensive library of tools and models to account for material behavior under various loading conditions allowing it to model gases, viscous materials, and solids. A particular feature of FLAG is that it incorporates material equations of state (EOS) in both analytical and tabular forms [20]. The EOS relates pressure, density, and internal energy. A material's EOS accounts for compressibility effects such as shock heating and density changes and is a critical component for accurately modeling shock wave propagation through materials [13]. FLAG has been previously used to study a variety of shock physics problems such as multiphase effects in shock-driven particle-gas instabilities [7], ejecta formation and transport [15], and Rayleigh-Taylor instabilities and spallation in simulated plate impact experiments [14,36]. FLAG has been verified and validated for a number of applications with simulations of the Noh problem [12], the Sedov problem [12], the Sod shock tube [12], and comparison to flyer plate experiments [32]. However, FLAG has not yet been used to model impact craters. In this work, we demonstrate that FLAG can be used for such problems through use of two verification and validation (V&V) problems common in planetary science. These problems were first presented by Pierazzo et al. to test several hydrocodes used for impact cratering simulations [30]. These V&V problems test both the early stages of impact cratering, dominated by thermodynamic properties rather than material properties, and crater evolution over

time, which is affected by the impactor and target materials along with gravity.

Code verification problems demonstrate that an algorithm solves the problem as intended, while code validation problems test its ability to match experimental data. The verification problem that we rely on here models an aluminum sphere impacting an aluminum target at 5 km/s and 20 km/s [30]. These aluminum-aluminum impact problems test a code's capability to capture key processes in the early stages of impact cratering, namely the contact and compression, and initial parts of the excavation stages that are driven by shock wave propagation. How well a code captures shock physics occurring during these early stages of impact cratering can be determined by calculating quantities such as the maximum shock pressure, shock pressure decay, temperature, and internal energy [30]. The verification simulations are run as strengthless because material strength plays a much larger role in the later stages of excavation and modification during a crater's formation, rather than the early stages which are studied with this problem [30]. The validation problem involves a laboratory experiment of a glass sphere impacting a water target, with data points measuring the evolution of the resulting crater radius and depth over time [30]. This validation problem tests a code's ability to model the kinematics of impact cratering, in addition to processes active in the later stages of crater formation such as material flow and ejection [30]. Although water does not display stress and damage in the same way as solid materials, the crater formation process is evident in the water's displacement. Together, these V&V problems allow for evaluation of both early and late stages of impact cratering, involving thermodynamic properties and material behavior under shock conditions. In addition to the V&V analysis, we conduct a mesh resolution study on FLAG using the aluminum-on-aluminum verification problem. We discuss the mesh resolution in terms of cells per projectile radius (cppr), following the same resolutions used by Pierazzo et al. [30].

As mentioned previously, these V&V problems were first used to test hydrocodes by Pierazzo et al. [30]. In this work, several hydrocodes that have been and continue to be used for impact cratering simulations were tested. While an in depth discussion of all of these methods is beyond the scope of this work, we briefly mention the key features of each code tested previously. Many of the previous codes studied were purely Eulerian formulations. While there are advantages of this method such as handling vorticity and shear without the risk of mesh tangling, it is more difficult to account for material strength, damage, and deformation than in Lagrangian approaches. ALE frameworks, as that used in FLAG, can be quite advantageous for impact cratering simulations because they can accommodate both vorticity and solid material properties. Of the eight codes tested by Pierazzo et al., half are multidimensional (1D, 2D, and 3D) Eulerian approaches: SOVA [34], ZEUS-MP2 [18], CTH [25], and RAGE [16]. These codes have different features valuable to cratering problems including framework that can accommodate multi-material problems, radiation hydrodynamics, and AMR. More similar to FLAG, iSALE [3, 22], ALE3D [33], and AUTODYN [4, 6] are all ALE codes. iSALE, however, is limited to 2D and was developed primarily to model fluids flow at a wide range of speeds. ALE3D is based on a finite element formulation rather than finite volume, and can address problems in 2 and 3 spatial dimensions. AUTODYN is perhaps the most similar in approach to FLAG as it is a coupled finite difference code with 2D and 3D capabilities with Lagrangian, Eulerian, ALE. AUTODYN additionally has smooth particle hydrodynamics (SPH) techniques, but it is expensive, and the source code is unavailable to users. Finally, SPH [5] was also included by [30] and is a multidimensional (1D, 2D, and 3D) SPH code without an underlying grid. For the verification problem, the hydrocodes tested by Pierazzo et al. [30] had an average peak shock pressure of 40.4 GPa in the 5 km/s vertical impact, with a low of 28.4 GPa (ZEUS-MP) and a high of 48 GPa (SOVA). In the 20 km/s vertical impact, the codes had an average peak shock pressure of 379 GPa, with a low of 335 GPa (ZEUS-MP) and a high of 411 GPa (SOVA) [30]. For the validation problem, the tested hydrocodes mostly had errors less than

15% in early time (less than 3.5 ms), with the exception of SOVA (25%) and ZEUS-MP (50%) [30]. Codes run at resolutions of 5 cppr underestimated the radius by 11% and depth by 14%, while codes run at resolutions of 10 cppr underestimated the radius by 7% and depth by 10% [30].

In this work we add FLAG to the list of hydrocodes that have been verified and validated for impact cratering simulations. FLAG combines many of the desirable features found in other codes commonly used in planetary science. For example, FLAG is massively parallel, conservative because of its finite volume approach, and is capable of solving problems in 1D, 2D, and 3D. Because of its parallelization, FLAG provides accurate results at reduced computational cost, lending itself to solving large problems like those found in planetary science [20]. Furthermore, FLAG has AMR capabilities, radiation hydrodynamics, allows the user to select the unit set, and can accommodate multi-material cells. Beyond these features, FLAG allows the user to choose from a variety of material models including a diverse set of EOS, both analytical and tabular, and various strength models describing plastic flow, work hardening, and damage in solid materials under shock conditions. Hence, FLAG offers a wide range of methods to capture the important physics at play in impact cratering.

2 Verification

To verify FLAG, we consider an aluminum impactor striking an aluminum target at impact velocities of 5 km/s and 20 km/s. The aluminum impactor is a sphere of diameter 1 km. Because the same material comprises both impactor and target, the particle velocity for the target and impactor are the same, and this value is equal to one-half the impact velocity [28]. We use Al-6061 for both the target and impactor material, and we determine the maximum pressure analytically for such an impact in one dimension to be 58.725 GPa for an impact velocity of 5 km/s and 506.25 GPa for an impact velocity of 20 km/s using Equation (1):

$$P = \rho_0 \left(C_0 + S U_p\right) U_p, \tag{1}$$

where P is the maximum pressure in GPa, ρ_0 is the initial density $\left(2.7 \text{ g/cm}^3\right)$, C_0 is the sound velocity at 0 pressure (5.35 mmμs), S is the linear EOS coefficient (1.34), and U_p is the particle velocity (1/2 impact velocity) [28].

We use FLAG to simulate these impacts in 1D, 2D, and 3D using Al-6061. For 1D simulations, we use a Mie-Grüneisen linear EOS for both target and impactor to better match the 1D analytic solution. For 2D and 3D simulations, we use a SESAME tabular EOS for both impactor and target [23] to stay consistent with the verification simulations in Pierazzo et al. [30]. We choose a resolution of 40 cppr, equivalent to a cell side length of 12.5 m. We use Eulerian (static) tracer particles located 200 m into the target for the 5 km/s impact and 685 m into the target for the 20 km/s impact. For artificial viscosity, we use a Barton model [24] with quadratic coefficient 2 and linear coefficient 0. We use free boundary conditions.

For the 1D simulations in FLAG, we use a projectile of 1 km and a target of 10 km, which allows us to measure peak pressure and shock pressure decay while avoiding boundary effects. For the EOS, we use 2700 kg/m^3 for the reference density, 890 J/kg/K for the specific heat, 5350 m/s for the sound speed, 2.0 for γ, and 1.34 as the linear coefficient [28]. We initialize the aluminum with density 2.7 g/cm^3 and an energy of 0 J. We use a pure Lagrangian approach for these simulations. For the 5 km/s impact, we obtain a maximum pressure of 63.68 GPa at the point of impact with a relative error of 8.44% with respect to the analytical solution. For the 20 km/s impact at the tracer particle, we obtain a maximum pressure of 521.93 GPa with a relative error of 3.01%. We attribute these deviations from the analytical solution to the effects of artificial viscosity, not included in

Equation (1). Figure 1 shows the pressure wave in the FLAG simulation 0.7 seconds after the 20 km/s impact.

Similarly in 2D, the aluminum projectile is a circle of diameter 1 km, and the aluminum target

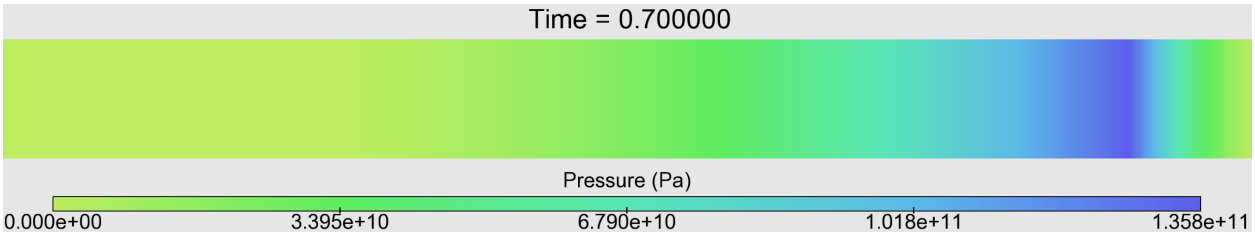

Figure 1: Pressure wave for FLAG simulation of 1D aluminum-on-aluminum 20 km/s impact 0.7 seconds after impact.

is a rectangle of length 25 km and width of 10 km. The surrounding material is air with length and width of 25 km and 23.5 km, respectively. The air is treated as a γ-law gas, with $\gamma = 1.4$. We initialize the air with a density of 1.2922×10^{-3} g/cm^3 at 273 K. For these simulations, we use FLAG's ALE capabilities to relax the mesh by geometry. Whenever a zone has an angle measure less than or equal to our specified threshold (15 degrees at first and 30 degrees when needed), we relax the mesh at that zone and up to three zones away. Simulated results for the stages of contact and compression, and excavation are shown in Figure 3 for the 5 km/s impact. In this case, we obtain maximum pressures at the tracer particle 200 m below impact ranging from 51.02 GPa to 55.77 GPa depending on mesh resolution, with deviations from the 1D analytic solution ranging from -13.12% to -5.15%. In comparison, the mean maximum pressure from the results of the eight codes tested by Pierazzo et al. [30] was 40.4 GPa with mean deviation from the analytic solution of -33.3%. We also examined the maximum pressure at a tracer particle at the point of impact, with values ranging from 56.29 GPa to 61.16 GPa and deviations from the analytic solution ranging from -4.15% to 4.15%, with a best case of 59.58 GPa and deviation of 1.46%. The cases with the smallest (in magnitude) errors in peak shock pressure at impact and 200 m into the target are listed in Table 1. Figure 2 shows the pressure wave of the FLAG simulation 0.161265 seconds after the 5 km/s impact.

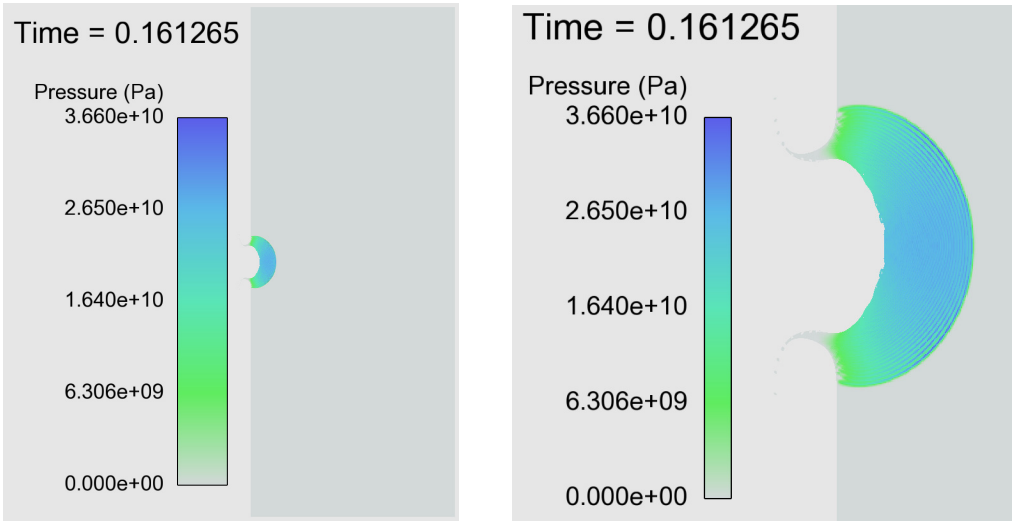

Figure 2: Pressure wave for FLAG simulation of 2D aluminum-on-aluminum 5 km/s impact 0.161265 seconds after impact for the entire target (left) and zoomed to show detail (right).

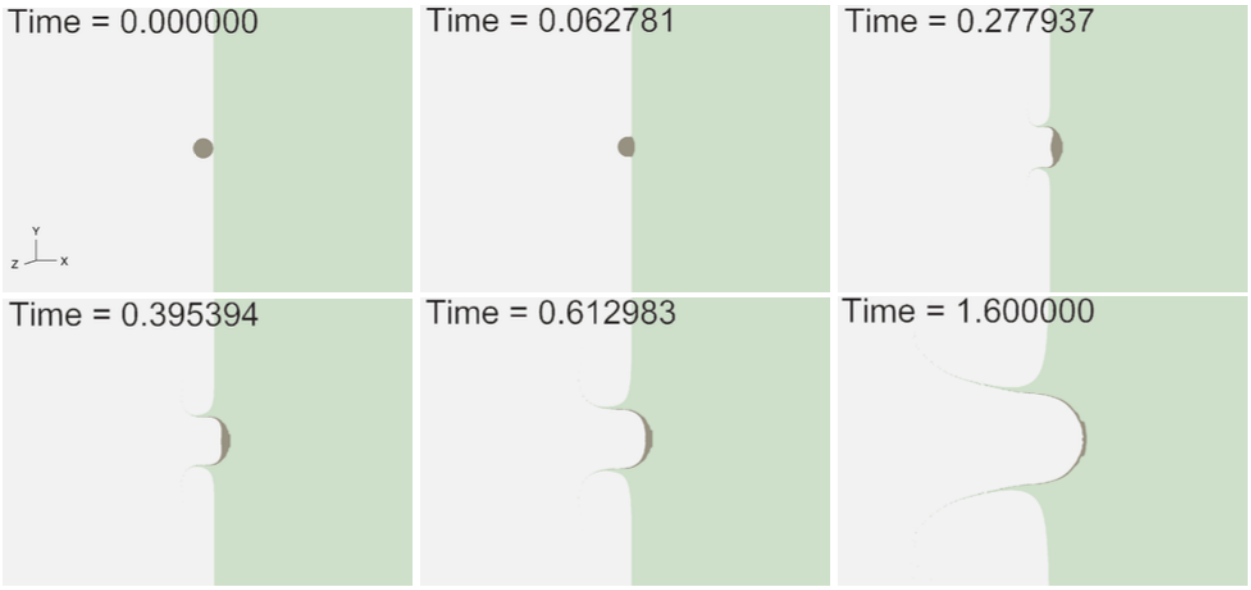

Figure 3: Stages of impact cratering in 2D FLAG simulation of an aluminum projectile (brown) impacting an aluminum target (green) at 5 km/s, zoomed in to show detail. The time is displayed in seconds.

For the 20 km/s impact, we obtain maximum pressures at tracer particles located 685 m into the target ranging from 388.64 GPa to 407.99 GPa depending on mesh resolution, with deviations from the 1D analytic solution ranging from -23.23% to -19.41%, which can be compared to a mean maximum pressure of 379.0 GPa with mean deviation from the analytic solution of -27.5% obtained by Pierazzo et al. [30]. We also measured the maximum pressure at impact and 200 m into the target, as in the 5 km/s impact, and found the highest pressure value 200 m into the target. At

this point, the maximum pressure of FLAG simulations ranged from 466.98 GPa to 494.81 GPa, depending on mesh resolutions, with deviations from the analytic solution ranging from -7.76% to -2.26%. The maximum pressure does not occur at the point of impact because we are measuring pressure with a static tracer particle. The higher impact velocity in this simulation results in the crater forming more quickly, and after the first time step, the point of impact no longer contains any target material. Using a Lagrangian tracer particle that moves with the material, we obtain the maximum pressure of 559.44 GPa, with a deviation from the 1D analytic solution of 10.51%, at the tracer particle initialized at the point of impact. The cases with the smallest (in magnitude) errors in peak shock pressure 200 m and 685 m into the target are listed in Table 1.

For the 3D FLAG simulations, the projectile is an aluminum sphere of diameter 1 km, and the

2D FLAG Simulation	1D Analytic Solution	FLAG	Pierazzo et al. Mean [30]
Maximum Pressure, 5 km/s 200 m into target	58.725 GPa	55.77 GPa	40.4 GPa
Percent Deviation from 1D Analytic	–	-5.15%	-33.3%
Maximum Pressure, 5 km/s point of impact	58.725	59.58 GPa	–
Relative Error	–	1.46%	–
Maximum Pressure, 20 km/s 685 m into target	506.25	407.99 GPa	379.0 GPa
Percent Deviation from 1D Analytic	–	-19.41%	-27.5%
Maximum Pressure, 20 km/s 200 m into target	506.25	494.81	–
Percent Deviation from 1D Analytic	–	-2.26%	–

Table 1: Maximum pressure of FLAG simulation of aluminum impacting aluminum from Eulerian (static) tracer particles located in the target. The results shown are from the tracer particle locations used by Pierazzo et al. [30] as well as the location of the maximum pressure obtained from 20 tracer particles approximately evenly spaced in the target.

target is an aluminum rectangular prism of length 25 km, width 10 km, and height 10 km. The surrounding material is air with length 25 km, width 23.5 km, and height 10 km. We simulated impact velocities of 5 km/s and 20 km/s and impact angles normal to the target surface and at a 45-degree angle. We ran all 3D simulations using a resolution of 5 cppr, resulting in approximately 8.3 million zones. We used FLAG's ALE capabilities to relax the mesh by geometry. We set our angle threshold to be 30, 45, or 60 degrees, as needed, and relaxed up to five zones away. For the 5 km/s normal impact, the maximum pressure occurred at the point of impact and measured 52.39 GPa with a deviation from the analytic solution of -10.79%. For the 20 km/s normal impact, the maximum pressure occurred 200 m into the target and measured 555.74 GPa with a deviation from the analytic solution of 9.78%. The 45-degree angle impacts do not have an associated analytic solution. Nevertheless, FLAG was able to complete these simulations, producing results consistent with impact craters. For these oblique impacts, the impactor breaks apart, with pieces of the impactor ending up more than 5 km outside the crater. The 5 km/s oblique impact simulation is shown in Figure 4. Figure 5 shows the pressure wave 0.732070 seconds after impact for the same

simulation. These simulations ran on 360 processors. The 5 km/s normal impact took about 5.75 hours for the pressure wave to propagate 10 km into the target, and the 20 km/s normal impact took about 6.5 hours.

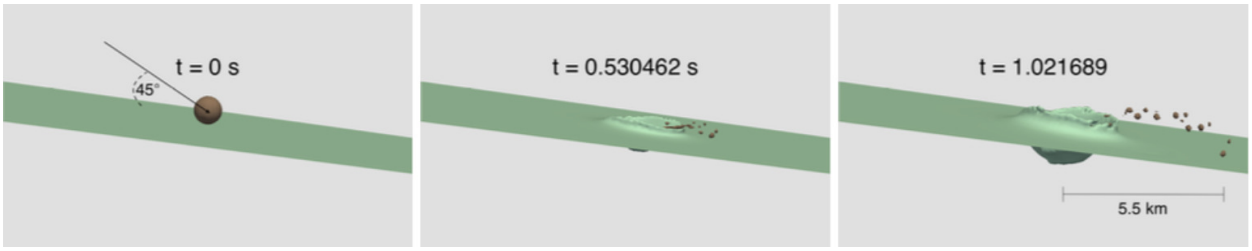

Figure 4: Visualization of 3D FLAG simulation of an aluminum sphere (brown) impacting an aluminum target (green) at 5 km/s at an impact angle of 45 degrees relative to the surface of the target.

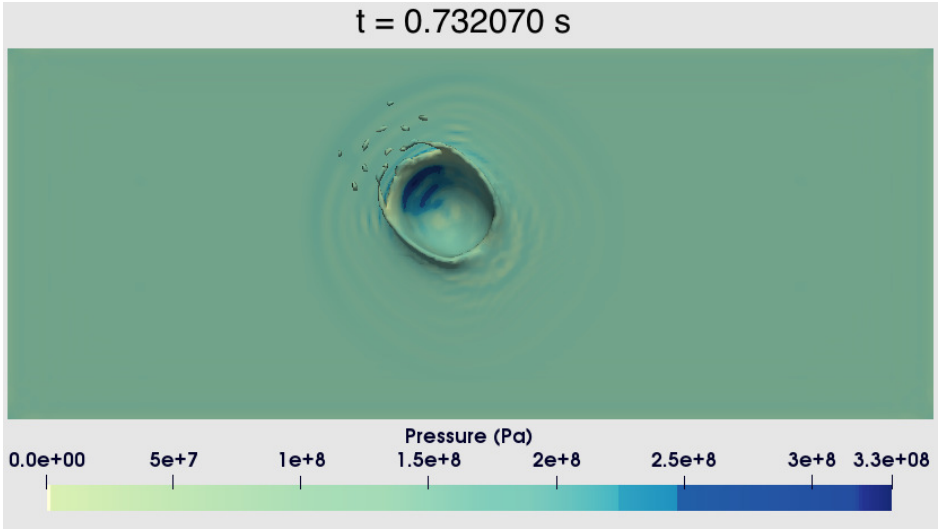

Figure 5: Pressure wave for FLAG simulation of 3D aluminum-on-aluminum 5 km/s 45-degree impact 0.732070 seconds after impact, shown looking into the crater from above.

One possible explanation for the lower percent deviation from the analytic solution with FLAG is its ALE capability, which reduces advection between cells. FLAG's interface reconstruction prevents numerical diffusion, which may also contribute to the lower errors in 1D and deviations from the 1D analytic maximum pressure in 2D and 3D. FLAG's Lagrange step also conserves internal energy [9, 10]. The advancement of interface reconstruction algorithms since the results from Pierazzo et al. [30] were first reported may help reduce such deviations. In the hydrocodes tested by Pierazzo et al [30], the best result for the maximum pressure was 48 GPa for the 5 km/s impact and 411 GPa for the 20 km/s impact, resulting in respective deviations of -18.26% and -18.82% relative to the 1D analytic solution. Running these simulations in FLAG resulted in respective errors of 8.44% and 3.01% in 1D and deviations from the 1D analytic solution of 1.46% and -2.26% in 2D and -10.79% and 9.78% in 3D. We attribute the higher error in the 1D 5 km/s simulation to artificial viscosity, which has a greater effect in lower velocity impacts. The different

EOSs used by Pierazzo et al. [30] likely contributed to the differences in results among the codes. One hydrocode tested by Pierazzo et al. [30], RAGE, also used a SESAME tabular EOS. Comparing these two codes, both implementing the SESAME EOS, we see a maximum pressure of 35.5 GPa in RAGE and 55.7 GPa in FLAG. The RAGE maximum pressure deviates from the 1D analytic by -39.55%, while the FLAG maximum pressure deviates from the 1D analytic by -5.15%. Thus, variations in the results among the codes are unlikely to be solely because of the choice of EOS.

2.1 Mesh Resolution Study

We conduct a mesh resolution study to determine at what resolutions FLAG converges for both impact velocities in the 2D aluminum-on-aluminum verification problem. To do this, we measured the shock pressure decay 10 km into the aluminum target by placing 20 approximately evenly spaced tracer points normal to the target surface, with the first located at the point of impact and the last located 10 km into the target. We recorded the pressure at each tracer point and plotted the maximum at each point. Mesh resolutions 5, 10, 20, and 40 cppr were tested, and the results are shown in Figure 6.

The shock pressure decay convergence of the hydrocodes tested by Pierazzo et al. [30] ranges from 20 cppr to 80 cppr for both impact velocities (see Figure 7), while FLAG appears to converge at 10 cppr for the 5 km/s impact velocity. For the 20 km/s impact velocity, FLAG performs well at 10 cppr, but the difference between the 10 cppr resolution and higher resolutions is evident. This may be a result of the increased material deformation that occurs at higher impact velocities, which requires more precise physics modeling. From this study, we can expect reasonable results using a 10 cppr resolution for lower impact velocities. For higher impact velocities, a higher resolution may be necessary, although 10 cppr may be sufficient in some cases. The convergence at coarser resolutions could be a result of how FLAG handles multi-material zones. FLAG keeps interfaces sharp so numerical diffusion is not an issue at interfaces. FLAG also does not enforce pressure-temperature equilibrium (PTE), which allows zones to have two distinct materials with distinct pressures and temperatures. This aides in the implementation of the EOS, as multi-material zones will deform based on the bulk moduli of the materials in the zone. These features allow FLAG to run a coarser mesh without numerical smearing, heating, and cooling [9, 10].

The lower resolution required for FLAG simulations means the computational cost of these simulations can be greatly reduced. Figure 8 shows the computation time for the pressure wave to propagate 10 km into the aluminum target. The highest resolution, 40 cppr, ran for approximately 28 hours, while the 10 cppr resolution simulation ran for approximately 25 minutes. For the 5 km/s impact, which converged at 10 cppr, using FLAG reduces the computational cost considerably. All 5 km/s impact simulations ran on 108 processors, and all 20 km/s impact simulations ran on 144 processors.

3 Validation

To validate FLAG for impact cratering, we use the same validation problem as in Pierazzo et al. [30], a laboratory experiment of glass impacting water. In this experiment, a glass sphere of diameter 2 mm impacts a rectangular target of dimension 76 cm $\times$ 38 cm $\times$ 23 cm. The target as a 1.25 cm aluminum liner, with the remaining volume filled with water. The impact velocity is 4.64 km/s.

Table 3 in Pierazzo et al. [30] shows the experimental data for crater radius and depth over time. The first data point occurs 0.191 ms after impact, and the last occurs 83.187 ms after impact. The crater obtains its maximum radius of 14.357 cm at the last data point and its maximum depth

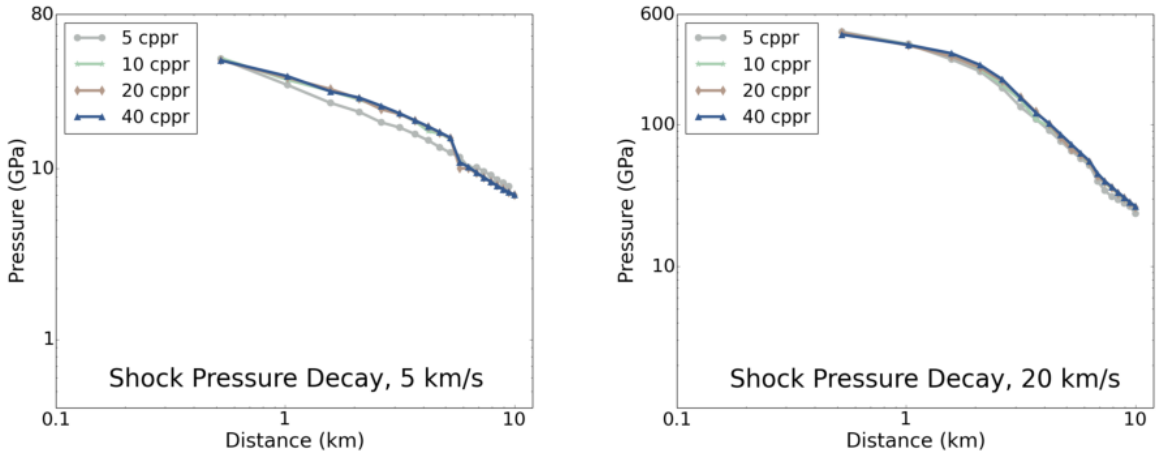

(a) (b)

Figure 6: Shock pressure decay of aluminum-on-aluminum verification problem with resolutions ranging from 5 to 40 cppr. (a) For an impact velocity of 5 km/s, FLAG appears to converge at a resolution of 10 cppr. (b) For an impact velocity of 20 km/s, FLAG appears to converge at a slightly higher resolution, although at 10 cppr, results may be sufficient in some cases.

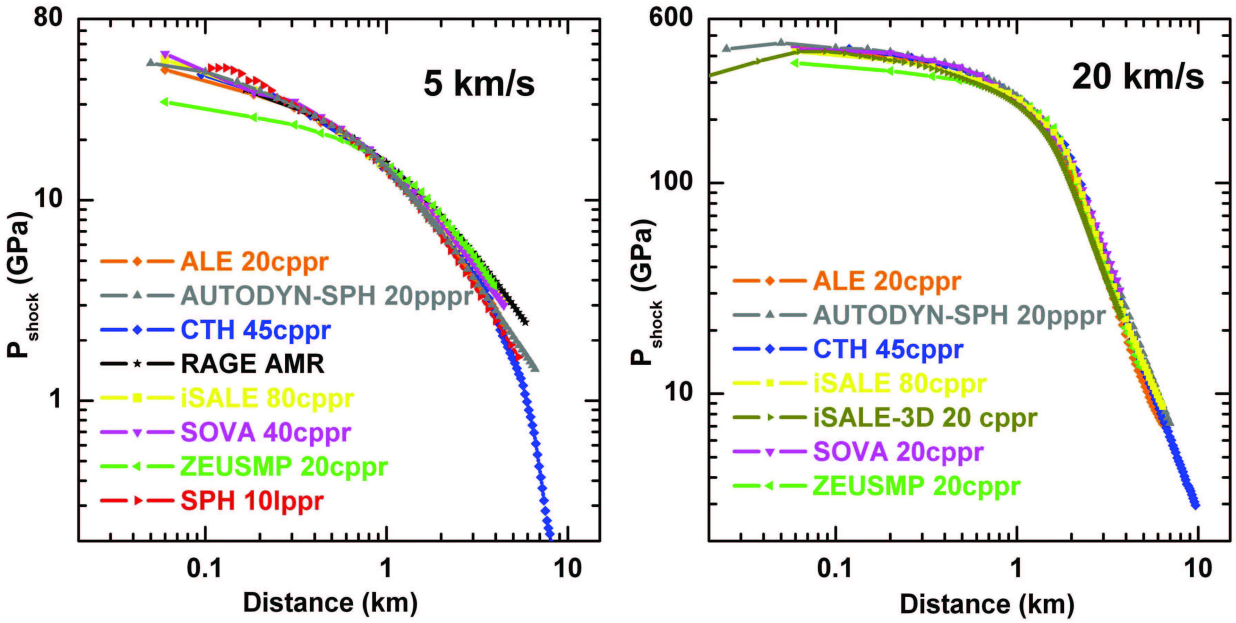

Figure 7: Fig. 1 from Pierazzo et al. [30], showing the shock pressure decay for a variety of tested hydrocodes for the aluminum-on-aluminum verification problem. As indicated by the figures, the majority of hydrocodes tested converged at 20 cppr or higher for the 5 km/s impact and at 20 cppr for the 20 km/s impact. This figure was approved for reproduction in this article by John Wiley and Sons under license number 4431420196094.

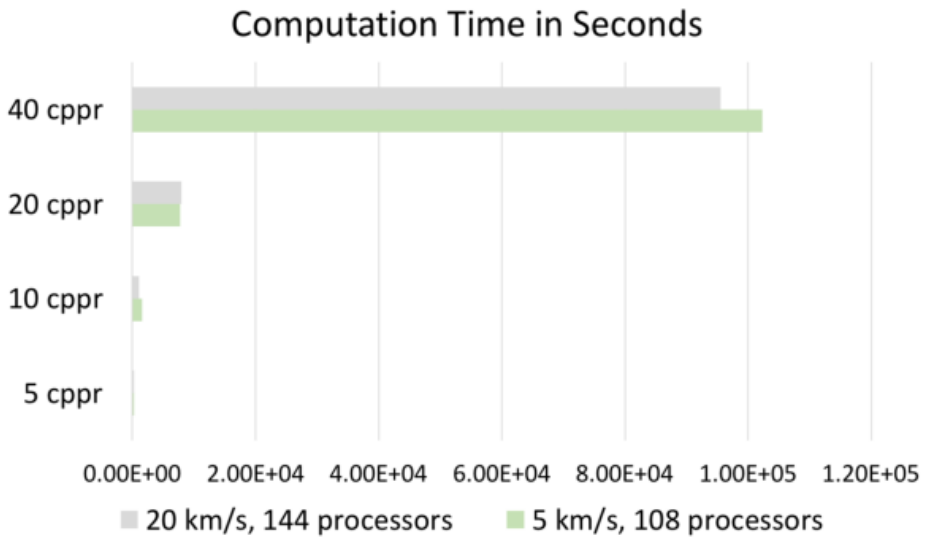

Figure 8: Computational times for FLAG simulations of the pressure wave propagation 10 km into target in an aluminum-on-aluminum verification problem. Simulations of the 5 km/s impact ran on 108 processors, and simulations of the 20 km/s impact ran on 144 processors.

of 12.1 cm at the penultimate data point, 65.335 ms after impact. These experimental data are displayed in Table 2.

Time (ms)	Radius (cm)	Depth (cm)
0.191	1.608	2.35
0.382	2.297	2.6
0.764	2.963	3.32
1.146	3.423	3.85
1.91	4.112	4.61
3.436	5.031	5.39
5.72	6.064	6.41
9.516	7.098	7.514
15.18	8.316	8.83
22.666	9.487	9.7
31.9	10.636	10.602
44.553	11.807	11.46
65.334	13.3	12.1
83.187	14.357	12.054

Table 2: Experimental data of crater radius and depth over time for the glass-on-water validation problem.

In order to avoid boundary effects in the validation problem, we use a computational mesh extending from 0 cm to 36.75 cm in the x direction and 1.25 cm to 1000 cm in the y direction. Because of the relatively small size of the glass impactor compared to the water target, we vary

the mesh resolution, using a finer mesh around the impactor and a coarser mesh far from impact. Our zone sizes range from 0.02 cm, equivalent to 5 cppr, at impact and 0.5 cm, equivalent to 0.2 cppr, at the boundaries. To further reduce the computational cost, we omit the aluminum liner and only include the right half of the water, choosing a 2D axisymmetric mesh. The glass impactor is a semicircle of radius 1 mm, positioned at the top of the water at initialization. The surrounding air extends to a height of 10 m to avoid top boundary effects. The 10 km boundary is high enough to prevent the ejected water from contacting the top boundary and splashing down into the crater while the crater is forming. We implement a constant gravity of -9.8 m/s^2 in the y direction. Figure 9 shows the problem at initial time.

This problem was considerably more computationally expensive than the aluminum verification problem. The small size of the impactor relative to the target limited the resolution size. Many of the hydrocodes tested by Pierazzo et al. [30] did not run to completion, and, instead, the authors displayed the crater dimensions that coincided with the first several experimental data points. Because of the computational intensity of the problem, we ran our simulation up to 9.516 ms, which encompasses 8 experimental data points. The hydrocodes tested by Pierazzo et al. [30] used resolutions ranging from 5 cppr to 20 cppr for this validation problem. We used a resolution of 5 cppr at the point of impact, which is the coarsest resolution tested in the verification problem. We chose such a coarse resolution because of the computational cost as well as the relative size of the impactor when compared to the target. Finer resolutions cause the adaptive time step to become arbitrarily small, prohibiting the simulation from providing meaningful results in an acceptable time frame. We ran our simulation in blocks of 10 hours on 360 processors. The first 10-hour run resulted in 7 data points. The second 10-hour run provided the 8th data point. An additional 11 10-hour runs produced no additional data points. In addition to the coarse resolution, we chose to run this simulation using FLAG's Eulerian mesh relaxer to prevent tangling during the excavation stage of crater formation.

(a) (b)

Figure 9: Glass into water validation problem at initial time of FLAG simulation showing the glass impactor (white), water target (blue), and surrounding air (grey). (a) The entire computational space for the glass into water validation problem. (b) Glass into water computational space, zoomed to show detail.

Because we used a coarse mesh, we anticipated that the FLAG simulations results would underestimate crater dimensions as had hydrocodes tested by Pierazzo et al. [30] when run with the 5 cppr resolution. At this resolution, these codes underestimated the crater radius by about 11% on average and underestimated the the depth by about 14% [30], while FLAG overestimated the crater depth by an average of 2.44% and underestimated the radius by an average of 6.2%. The overestimation of the depth could be a result of the axisymmetric boundary condition, which tends to result in jets that are too thin and penetrate too far because movement is allowed in only one direction and will be dominated by gravity. We measured the crater radius at 0.1 cm below the initial water line, and we measured the crater depth 0.3 cm to the right of the crater's center. The results of the FLAG simulation as well as the corresponding experimental data are listed in Table 3 and shown in Figure 10.

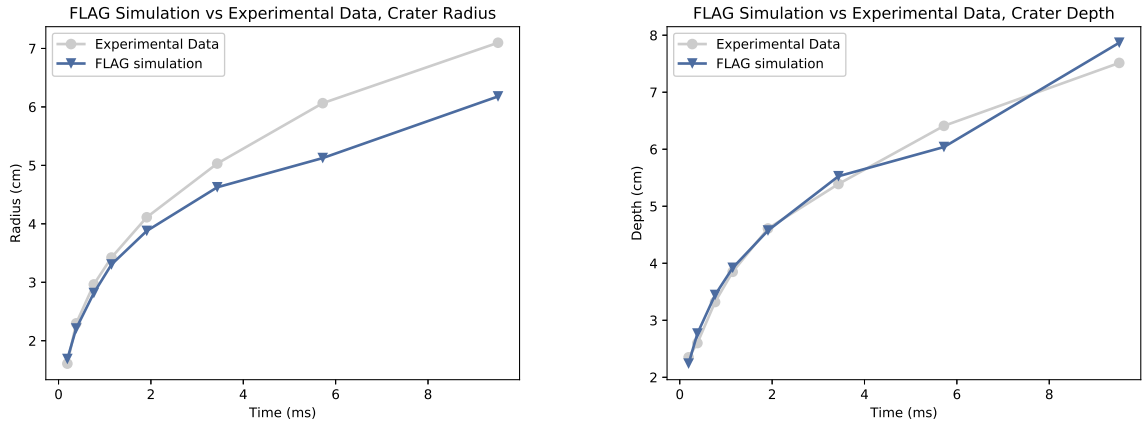

(a) (b)

Figure 10: Experimental data and FLAG simulation results for the glass-on-water validation problem for crater radius (left) and crater depth (right) over time. The FLAG simulation had an average relative error of about -6.2%, and the depth had an average relative error of 2.44%.

Time (ms)	Experimental Radius (cm)	FLAG Radius (cm)	Relative Error	Experimental Depth (cm)	FLAG Depth (cm)	Relative Error
0.191	1.608	1.68713	4.92%	2.35	2.23934	-4.71%
0.382	2.297	2.20879	-3.84%	2.6	2.7669	6.42%
0.764	2.963	2.81574	-4.97%	3.32	3.44335	3.72%
1.146	3.423	3.30393	-3.48%	3.85	3.91973	1.81%
1.91	4.112	3.87845	-5.68%	4.61	4.57374	-0.79%
3.436	5.031	4.62491	-8.07%	5.39	5.52639	2.53%
5.72	6.064	5.12498	-15.49%	6.41	6.03864	5.79%
9.516	7.098	6.179	-12.95%	7.514	7.868	4.71%

Table 3: FLAG simulation results of glass-on-water impact validation problem with relative errors, round to two decimal places. The codes tested by Pierazzo et al. had an average error of about -11% for radius and -14% for depth [30].

The depth-to-radius ratios of both the FLAG simulations and experimental data are listed in Table 4 and shown in Figure 11a. The resulting FLAG simulation crater 1.145 ms after impact, reflected about the axis of symmetry, is shown in Figure 11b.

We implemented FLAG's subcycling capability on this validation problem in order to obtain

Time (ms)	Experimental Depth/Radius	FLAG Depth/Radius	Relative Error
0.191	1.461	1.327	-9.17%
0.382	1.132	1.253	10.69%
0.764	1.120	1.223	9.20%
1.146	1.125	1.186	5.42%
1.91	1.121	1.179	5.17%
3.436	1.071	1.195	11.58%
5.72	1.057	1.178	11.45%
9.516	1.059	1.273	20.21%

Table 4: FLAG simulation results of the depth-to-radius ratio compared to experimental data for the glass-on-water validation problem.

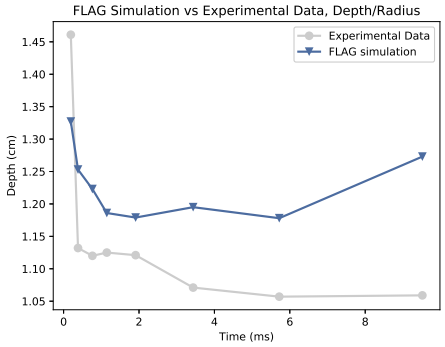

(a)

(b)

Figure 11: (a) Depth/Radius ratio of experimental data and FLAG simulation for the glass-on-water validation problem. (b)
FLAG simulation crater 1.146 ms after a 2 mm diameter glass sphere impacts a water target at 4.64 km/s, reflected about the axis of symmetry.

more accurate results without increasing the mesh resolution, which proved too computationally intensive. Subcycling allows for extra iterations during the mesh remapping process. This method provided fewer data points for the same computational time, but the results for the early simulation time resulted in errors as low as -0.17%. The average error for the crater radius was -5.04%, and the average error for the crater depth was -5.03%. Subcycling resulted in a nearly identical average error for both the crater radius and crater depth.

4 Conclusions

Based upon our verification and validation problems, we conclude that the FLAG hydrocode can be used for impact cratering simulations. We have shown through our verification problem that FLAG captures the important shock dynamics in early stages of crater formation, and we have shown through our validation problem that FLAG matches experimental data with a low relative error. These problems have been accepted by the planetary science community as adequate tests for hydrocodes. FLAG simulated the verification problem of aluminum into aluminum producing maximum pressure values close to the analytical solutions, with errors as low as 4.2% compared to a mean error of 33.3% in results from the hydrocodes tested by Pierazzo et al. [30]. The mesh resolution study demonstrated FLAG's potential to handle impact cratering problems at coarser resolutions than other hydrocodes, reducing the computational time from 28 hours to 25 minutes. The validation problem of a glass impactor and water target was used to measure FLAG's ability to match experimental data. The FLAG simulation of this problem gave promising results despite a very coarse resolution, with errors an order of magnitude better than other hydrocodes tested at the same resolution [30]. FLAG's variety of EOS options, multiple material models, ALE capabilities, and relatively good run times contribute to its accurate modeling for both theoretical and experimental physical problems. These V&V problems tested FLAG's Lagrange, ALE, and Eulerian features, demonstrating FLAG's reliability for a variety of problem approaches.

5 Acknowledgments

The authors gratefully acknowledge the Lagrangian Applications Project code team for providing valuable assistance. This work was supported by the Advanced Simulation and Computing (ASC)–Integrated Codes (IC) program and the ASC–Threat Reduction (TR) program at Los Alamos National Laboratory. Los Alamos National Laboratory, an affirmative action/equal opportunity employer, is operated by Triad National Security, LLC, for the National Nuclear Security Administration of the U.S. Department of Energy under contract 89233218NCA000001.

References

[1] Michael F. A'Hearn, M.J.S. Belton, W.A. Delamere, J. Kissel, K.P. Klaasen, L.A. McFadden, K.J. Meech, H.J. Melosh, P.H. Schultz, J.M. Sunshine, et al. Deep Impact: Excavating Comet Tempel 1. *Science*, 2005.

[2] Thomas J. Ahrens and Alan W. Harris. Deflection and fragmentation of near-Earth asteroids. *Nature*, 360(6403):429, 1992.

[3] A.A. Amsden, H.M. Ruppel, and C.W. Hirt. SALE: A Simplified ALE Computer Program for Fluid Flow at All Speeds. Technical report, Los Alamos Scientific Lab., 1980.

[4] ANSYS Autodyn. Theory Manual Revision 4.3. *Century Dynamics, Concord, CA*, 2005.

[5] Willy Benz and Erik Asphaug. Simulations of brittle solids using smooth particle hydrodynamics. *Computer Physics Communications*, 87(1-2):253–265, 1995.

[6] N.K. Birnbaum, M.S. Cowler, M. Itoh, M. Katayama, and H. Obata. Autodyn–an interactive non-linear dynamic analysis program for microcomputers through supercomputers. In *Transactions of the 9th international conference on structural mechanics in reactor technology. Vol. B*, 1987.

[7] W.J. Black, N.A. Denissen, and J.A. McFarland. Evaporation Effects in Shock-Driven Multiphase Instabilities. *Journal of Fluids Engineering*, 139(24):071204, 2017.

[8] M.B.E. Boslough and D.A. Crawford. Low-altitude airbursts and the impact threat. *International Journal of Impact Engineering*, 35(12):1441–1448, 2008.

[9] D. Burton. Connectivity Structures and Differencing Techniques for Staggered-Grid Free-Lagrange Hydroynamics. Technical Report UCRL-JC-110555, Lawrence Livermore National Laboratory, Livermore, CA, 1992.

[10] D. Burton. Consistent Finite-Volume Discretization of Hydrodynamic Conservation Laws for Unstructured Grids. Technical Report UCRL-JC-118788, Lawrence Livermore National Laboratory, Livermore, CA, 1994.

[11] D. Burton. Multidimensional Discretization of Conservation Laws for Unstructured Polyhedral Grids. Technical Report UCRL-JC-118306, Lawrence Livermore National Laboratory, Livermore, CA, 1994.

[12] D. Burton, N.R. Morgan, M.R.J. Charest, M.A. Kenamond, and J. Fung. Compatible, energy conserving, bounds preserving remap of hydrodynamic fields for an extended ALE scheme. *Journal of Computational Physics*, 355:492–533, 2018.

[13] Gareth S. Collins. An Introduction to Hydrocode Modeling. *Applied Modelling and Computation Group, Imperial College London*, pages 2–11, 2002.

[14] J.H. Cooley, R.T. Olson, and D. Oro. Modeling and analysis of high-explosive driven perturbed plate experiments at Los Alamos. *Journal of Physics: Conference Series*, 500:152003, 2014.

[15] Jimmy Fung, Alan K. Harrison, Shirish Chitanvis, and Jeremy Margulies. Ejecta source and transport modeling in the FLAG hydrocode. *Computers & Fluids*, 83:177–186, 2013.

[16] Michael Gittings, Robert Weaver, Michael Clover, Thomas Betlach, Nelson Byrne, Robert Coker, Edward Dendy, Robert Hueckstaedt, Kim New, W. Rob Oakes, et al. The RAGE radiation-hydrodynamic code. *Computational Science & Discovery*, 1(1):015005, 2008.

[17] William K. Hartmann and Gerhard Neukum. Cratering Chronology and the Evolution of Mars. In *Chronology and Evolution of Mars*, pages 165–194. Springer, 2001.

[18] John C. Hayes, Michael L. Norman, Robert A. Fiedler, James O. Bordner, Pak Shing Li, Stephen E. Clark, Mordecai-Mark Mac Low, et al. Simulating Radiating and Magnetized Flows in Multiple Dimensions with ZEUS-MP. *The Astrophysical Journal Supplement Series*, 165(1):188, 2006.

[19] Paul O. Hayne, Benjamin T. Greenhagen, Marc C. Foote, Matthew A. Siegler, Ashwin R. Vasavada, and David A. Paige. Diviner Lunar Radiometer Observations of the LCROSS Impact. *Science*, 330(6003):477–479, 2010.

[20] James L. Hill. *User's Manual for FLAG version 3.6.0.* The Lagrangian Applications Project, Los Alamos National Laboratory, January 2017. LA-CP-17-20057.

[21] K.A. Holsapple. The Scaling of Impact Processes in Planetary Sciences. *Annual Review of Earth and Planetary Sciences*, 21(1):333–373, 1993.

[22] B.A. Ivanov, D. Deniem, and G. Neukum. Implementation of dynamic strength models into 2D hydrocodes: Applications for atmospheric breakup and impact cratering. *International Journal of Impact Engineering*, 20(1-5):411–430, 1997.

[23] Stanford P. Lyon and James D. Johnson. SESAME: The Los Alamos National Laboratory Equation of State Database. Technical report, Los Alamos National Laboratory, 1992. LA-UR-92-3407.

[24] L.G. Margolin. A centered artificial viscosity for cells with large aspect ratio. *NASA STI/Recon Technical Report N*, 89, 1988.

[25] J. Michael McGlaun, S.L. Thompson, and M.G. Elrick. CTH: a three-dimensional shock wave physics code. *International Journal of Impact Engineering*, 10(1-4):351–360, 1990.

[26] H. Jay Melosh. Impact cratering: A geologic process. *Oxford University Press (Oxford Monographs on Geology and Geophysics, No. 11), 1989, 253 p.*, 11, 1989.

[27] H. Jay Melosh. *Planetary Surface Processes*, volume 13. Cambridge University Press, 2011.

[28] Marc A. Meyers. *Dynamic Behavior of Materials*. John Wiley & Sons, 1994.

[29] Michael C Nolan, Erik Asphaug, H Jay Melosh, and Richard Greenberg. Impact Craters on Asteroids: Does Gravity or Strength Control Their Size? *Icarus*, 124(2):359–371, 1996.

[30] E. Pierazzo, N. Artemieva, E. Asphaug, E.C. Baldwin, J. Cazamias, R. Coker, G.S. Collins, D.A. Crawford, T. Davison, D. Elbeshausen, et al. Validation of numerical codes for impact and explosion cratering: Impacts on strengthless and metal targets. *Meteoritics & Planetary Science*, 43(12):1917–1938, 2008.

[31] Catherine S. Plesko. *Automated feature detection and hydrocode modeling of impact-related structures on Mars*. University of California, Santa Cruz, 2009.

[32] Christina A Scovel and Ralph Menikoff. A verification and validation effort for high explosives at Los Alamos National Lab. In *AIP Conference Proceedings*, volume 1195, pages 169–172. AIP, 2009.

[33] R. Sharp. Users Manual for ALE3D: An Arbitrary Lagrange/Eulerian 3D Code System. *Lawrence Livermore National Laboratory*, 2005.

[34] V.V. Shuvalov. Multi-dimensional hydrodynamic code SOVA for interfacial flows: Application to the thermal layer effect. *Shock Waves*, 9(6):381–390, 1999.

[35] A.M. Stickle, E.S.G. Rainey, M. Bruck Syal, J.M. Owen, P. Miller, O.S. Barnouin, and C.M. Ernst. Modeling impact outcomes for the Double Asteroid Redirection Test (DART) mission. *Procedia Engineering*, 204:116–123, 2017.

[36] D.L. Tonks, D.L. Paisley, P.D. Peralta, S.R. Greenfield, D.D. Byler, S. Luo, D.C. Swift, and A.C. Koskelo. Spallation damage in copper with columnar grains. *AIP Conference Proceedings*, 955:605–608, 2007.